Numerical evaluation of a muon tomography system for imaging defects in concrete structures.

Sridhar Tripathy

Saha Institute of Nuclear Physics, Kolkata, India

Homi Bhabha National Institute, Mumbai, India

Muon Scattering tomography (MST)

- High-energy (mean ~4 GeV), massive (~105 MeV/c^2)
- Based on multiple coulomb scattering.
- Applications: Imaging large structures, volcanos, examining cargo containers, nuclear waste etc.
- Natural background Non-hazardous unlike x-ray and gamma ray.

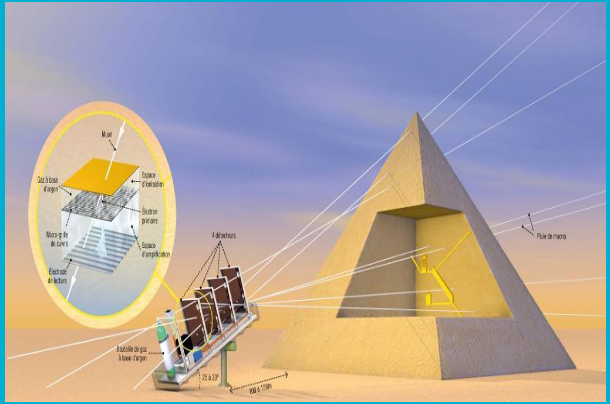

Scan Pyramid Project,CEA

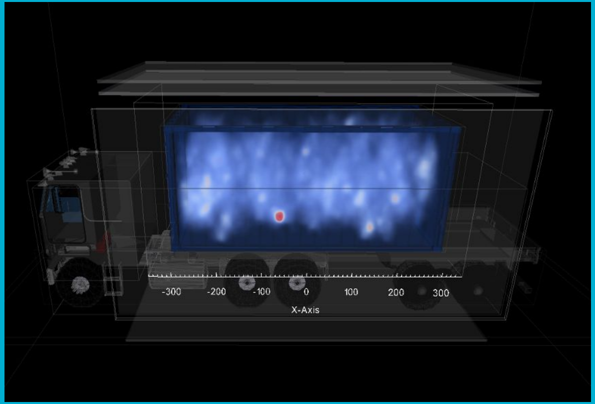

http://mutomweb.pd.infn.it:5210/

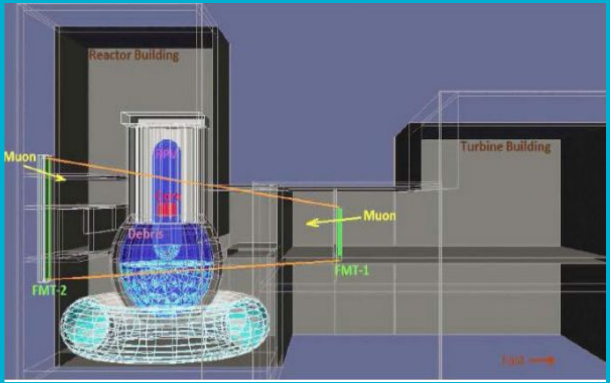

Fukushima Daichi Imaging unit (LANL)

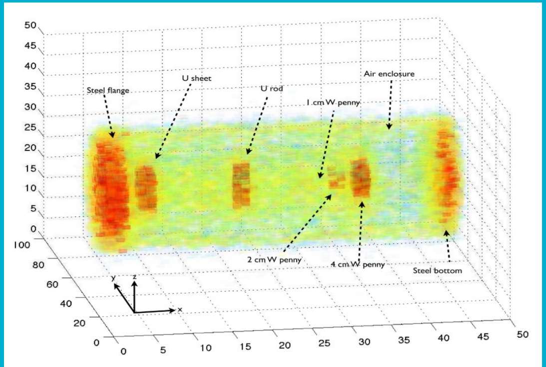

Simulation of Nuclear waste drum (Univ. of Bristol)

Motivation: Imaging Concrete Structures

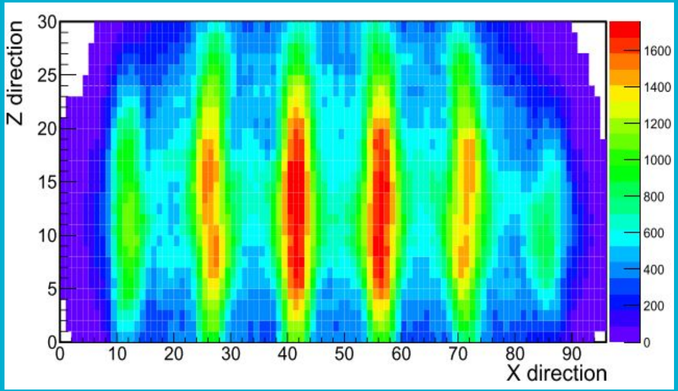

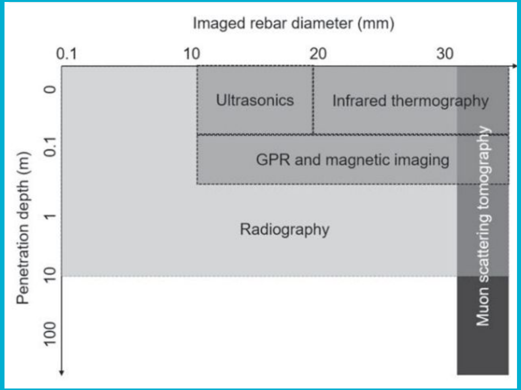

(a) Images of iron rebars embedded in concrete. (b) Comparison of MST with other NDE techniques. Ref: *M. Dobrowolska et al., Smart Mater. Struct. 29 055015 (2020)*

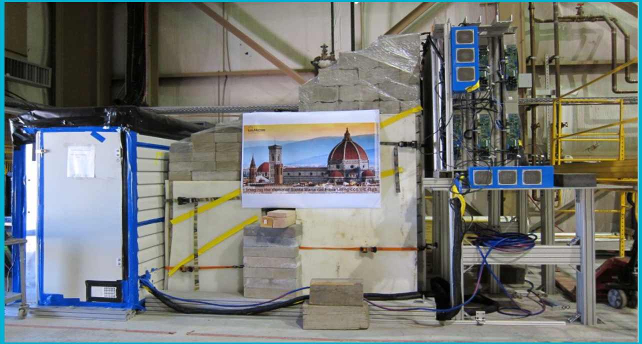

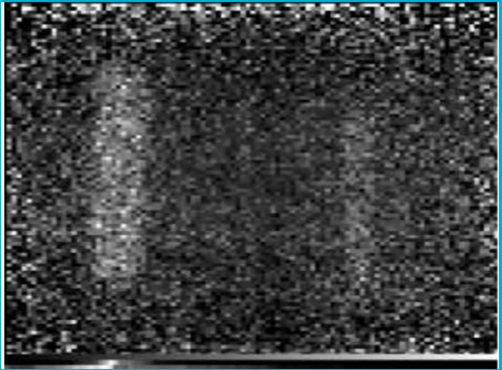

(a) Images of iron bars behind mockup walls. (b) Comparison of MST with other NDE techniques. Ref: *E. Guardincerri et al., AIP Advances 6, 015213 (2016)*

- Due to high-penetrating power and less-interacting nature, muons to pass through upto ~100m.
- MST has been used for imaging reinforced cement concrete (RCC) structures by computation as well as experiment
- In this work, we have tried go one step beyond to use MST for health monitoring of concrete structures based on portal imaging to image certain defects.
- Limitation & capability of the imaging of concrete defects with MST have been studied.

Simulation geometry

- 6 detectors, area calibrated according to the ROI.
- Parallel plate gaseous detectors.
- Detector separation: 7 cm
- CRY generator for muons
- Track reconstruction algorithm: Point of Closest Approach (PoCA)
- 2D image reconstruction
- Analysis based on scattering angle (ϴ)
- 30 days equivalent of muon exposure
- Detector spatial resolution: 200 um

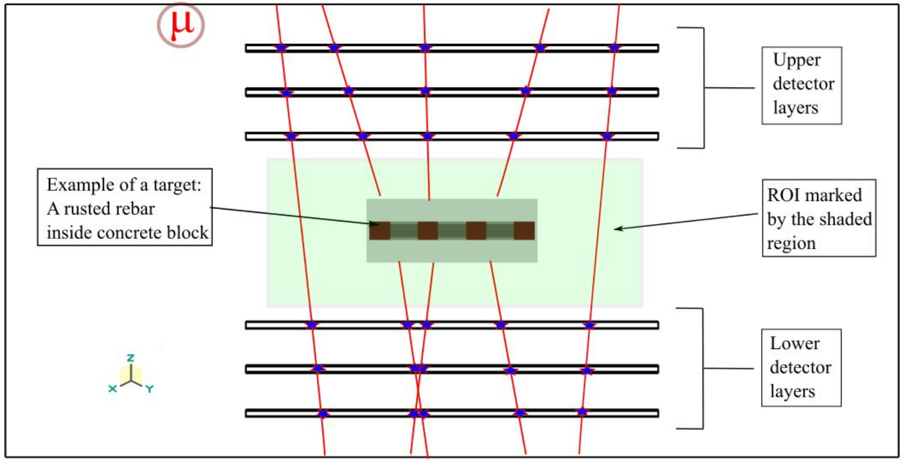

Schematic diagram of the simulated geometry.

Description of problem: Rusted Rebar

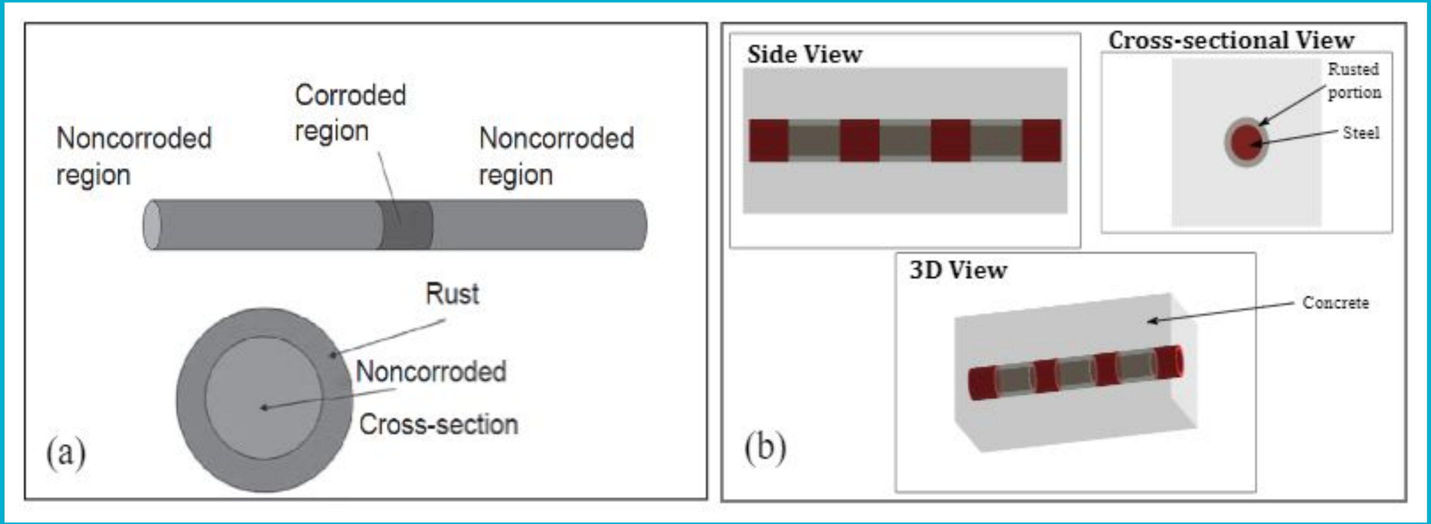

(a) Schematic diagram of partially corroded rebar. (reproduced from DOI: 10.1016/B978-1-78242-327-0.00009-X) (b) Image of the simulated geometry in GEANT4.

- Concrete Volume: 25X10X10 cm^3
- Rebar Dimension: length=24 cm, diameter=3 cm.
- Rust Thickness: 2.25 mm, 4.5 mm.
- Rust (Fe_2O_3) density 5.25 g/cc, Steel 7.87 g/cc, Concrete 2.3 g/cc

Description of problem: CFST Defect

Concrete Filled Steel Tubes (CFST)

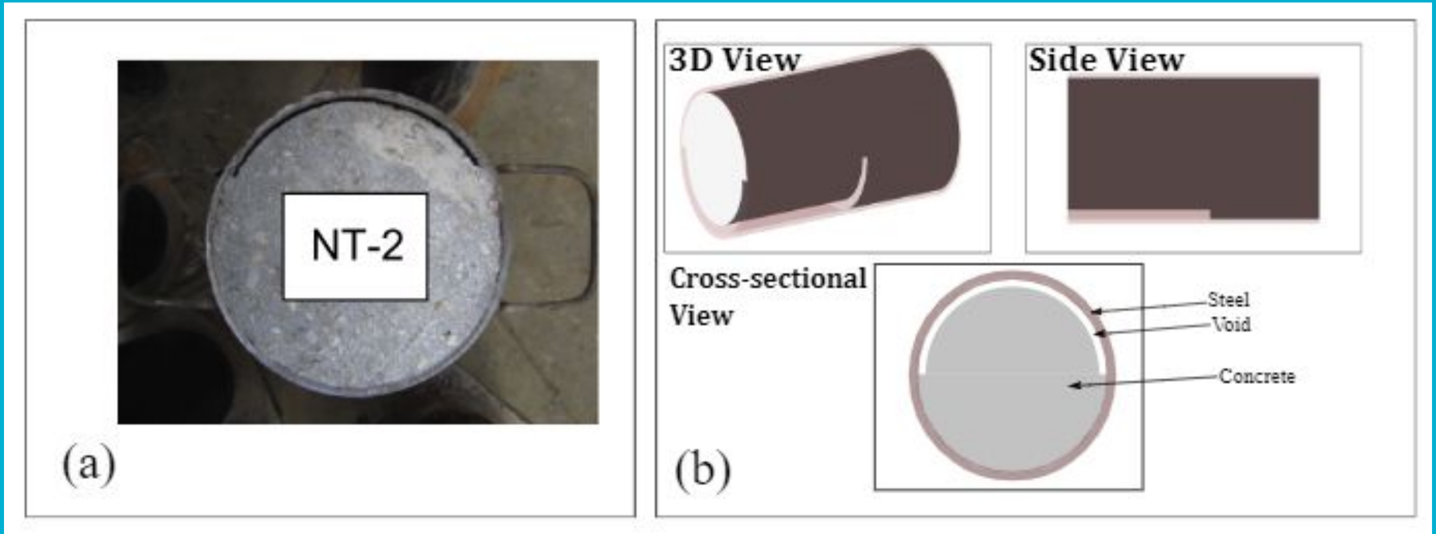

(a) CFST constructed deliberately with a circumferential void (reproduced from W. Dong et. al., Construction and Building Materials 128 (2016) 154–162) (b) Three views of simulated geometry in GEANT4.

- Important element in pillars of bridges and high-rise buildings
- CFST diameter: 16 cm,length: 30cm, Steel covering: 5 mm
- Void Thickness: 7 mm, 10 mm.
- CFST has been kept along the axial direction and defect is placed side-on for best cosmic exposure.

Description of problem: Void in Concrete Decks

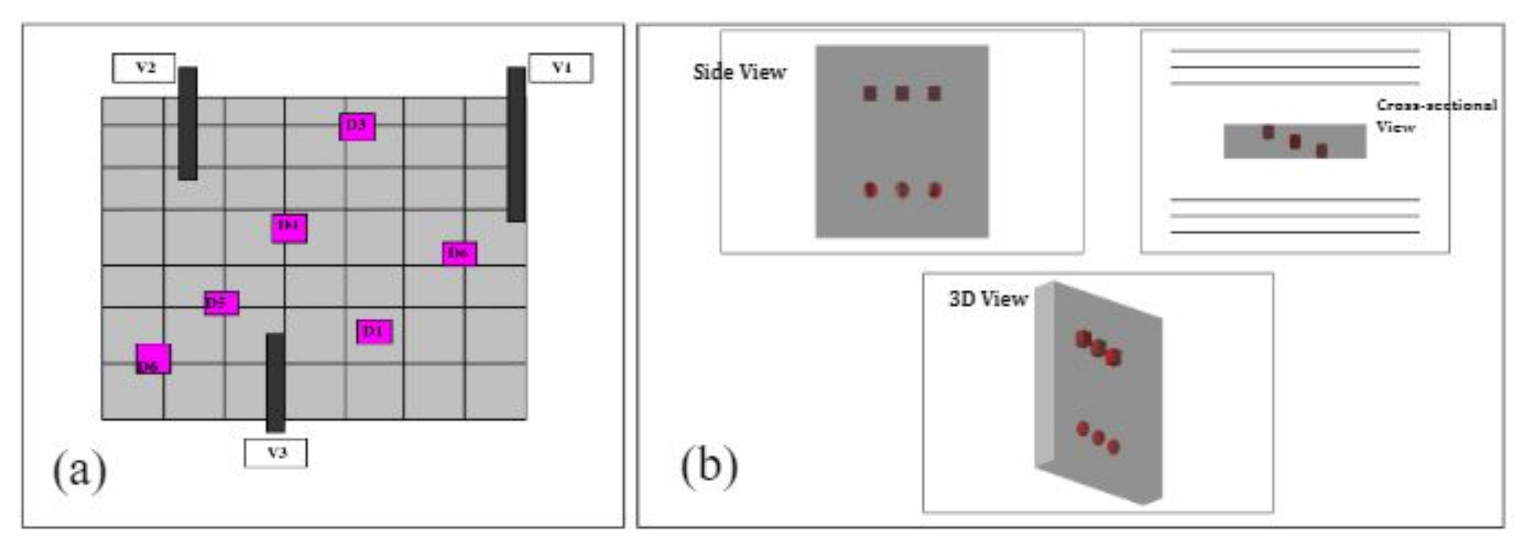

(a) Schematic diagram of concrete deck used in I. Abdel-Qader et al. / NDT&E International 41 (2008) 395–405 (b) Image of the simulated geometry in GEANT4.

- Concrete Volume: 80X80X15 cm^3
- Void Type: spherical and cubical
- Void Size: spherical: diameter:6.74 cm, 5.64 cm, cubical: side 6cm, 5cm
- Voids are placed in three different depth in Z (4cm, 8cm, 12 cm)

Detection Methodology:t-statistics

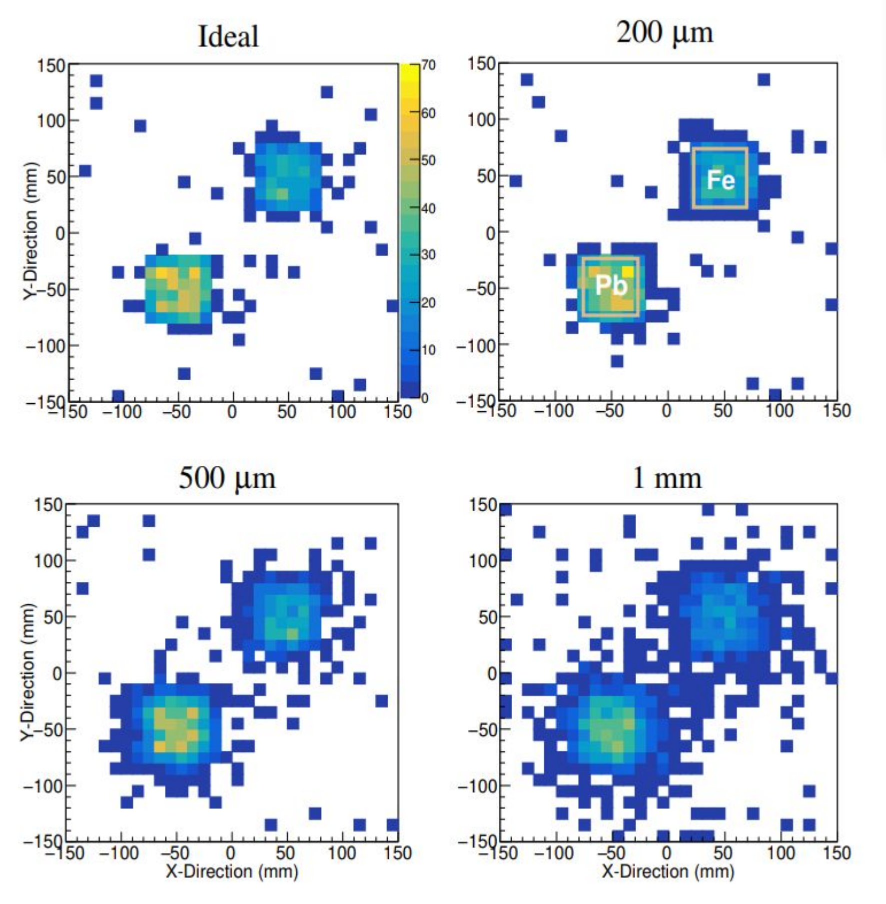

$$t = \frac{\mu_1 - \mu_2}{s_v \left[\frac{1}{n_1} + \frac{1}{n_2}\right]}$$

with $s_v = \sqrt{\left[\frac{(n_1-1){s_1}^2 + (n_2-1){s_2}^2}{n_1+n_2-2}\right]}$

Test	t-value	p-value
Ideal vs 200 μm	-0.37	**0.71**
Ideal vs 500 μm	-1.43	**0.15**
Ideal vs 1 mm	-3.60	8e-4

- ➔ t-statistics is widely accepted for checking if means of two distributions are equal.
- ➔ The test begins with assuming the null hypothesis that the data from the two images are identical.
- ➔ This test has been applied to compare Fe and Pb cubes are different resolutions.
- ➔ It has been used to compare images of without-defect concrete structures to the defective ones.

S. Tripathy et al.,JINST 15 (2020) 06, P06029

Detection Methodology:Pattern Recognition Method (PRM)

Image based on Fe Sample

Image based on Pb Sample

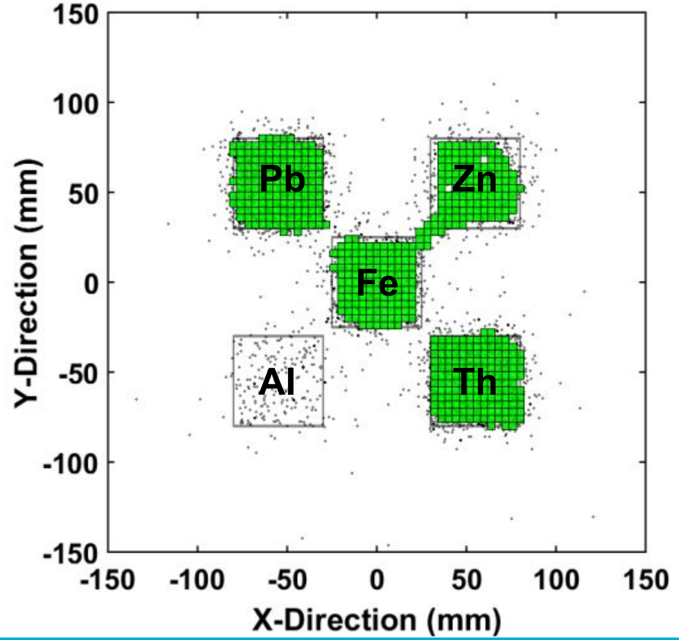

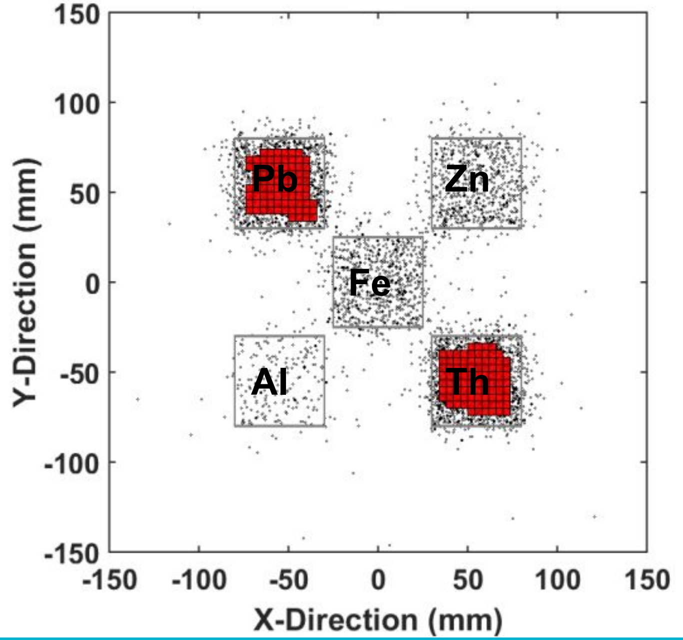

The **PRM** with Fe misses Al and identifies others

The **PRM** with Pb misses all with scattering parameter less than lead

S. Tripathy et al., JINST 15 (2020) 06, P06029

Detection Methodology:Pattern Recognition Method (PRM)

- ➔ A PRM-score has been introduced to evaluate similarity and quality of imaging.
- ➔ The PRM-score for a given case is the ratio of the number of pixels found void in the defected case (test case), '*m*' to the total pixels found in the non-defected case (sample), '*n*' in terms of the step '*δn*'.
- ➔ The step '*δn*' is a random relative error that may arise when PRM is repeatedly applied on the image.

$$\delta n = \frac{\sqrt{n}}{n} \text{ or } \frac{1}{\sqrt{n}}$$

$$\text{PRM-score} = \frac{m}{n \times \delta n}$$

- ➔ The interpretation of PRM-score is: How many steps the test image is from the without-defect case. $2\delta n$ random considered as benchmark for discrimination.

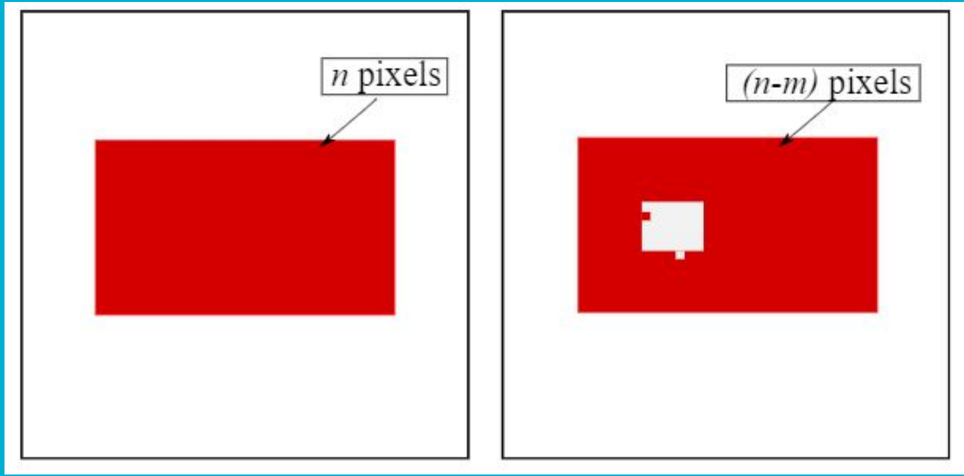

A mock-up diagram explaining two images after applying PRM, one without-defect and other defective.

Results: Rusted Rebar

- ❏ Scattering hit-image, and PRM images for without-defect, and 2 defective rebar cases.
- ❏ Scattering parameter has been shown in the color scale.
- ❏ The steel rebar and its defects are identified.
- ❏ The 15% rebar has been identified with > 2σ with t-statistics but unable to reach $2\delta n$ mark. table

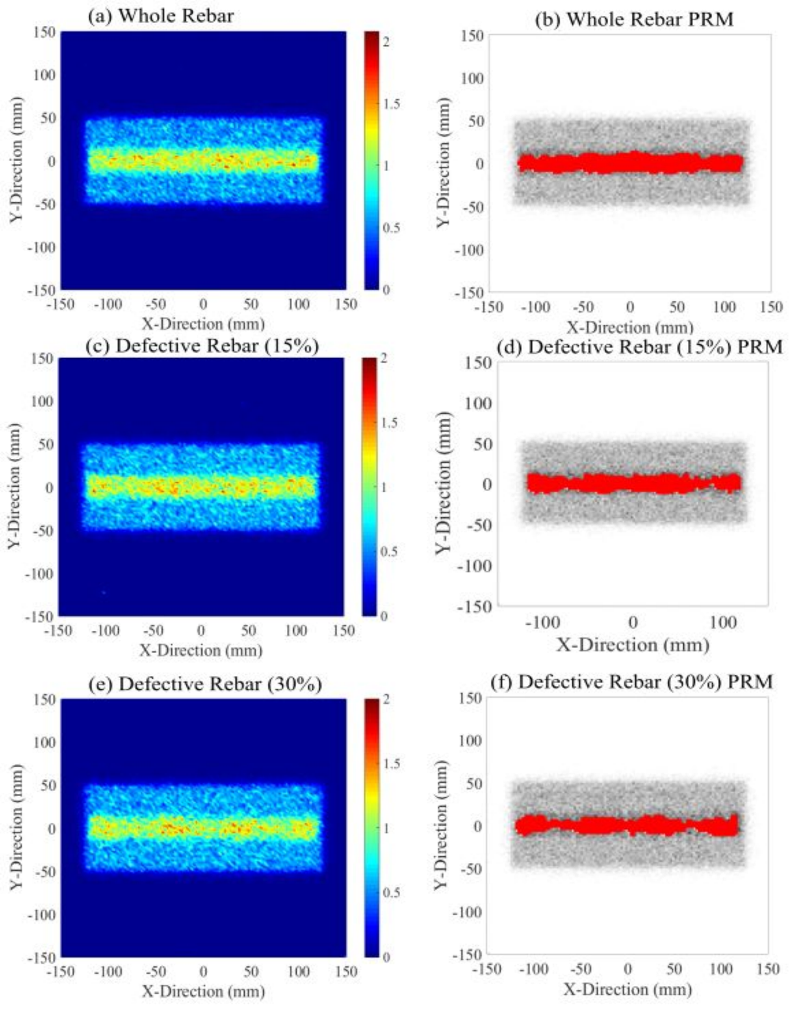

Results: CFST Defect

- Case of void in concrete with wrapped around steel
- Voids found closer to the edges
- Extent of defect not accurate
- Both 7mm and 10mm voids are identified
- The defects have been identified with > 3σ with t-statistics and > $2\delta n$ from the without-defect case. table

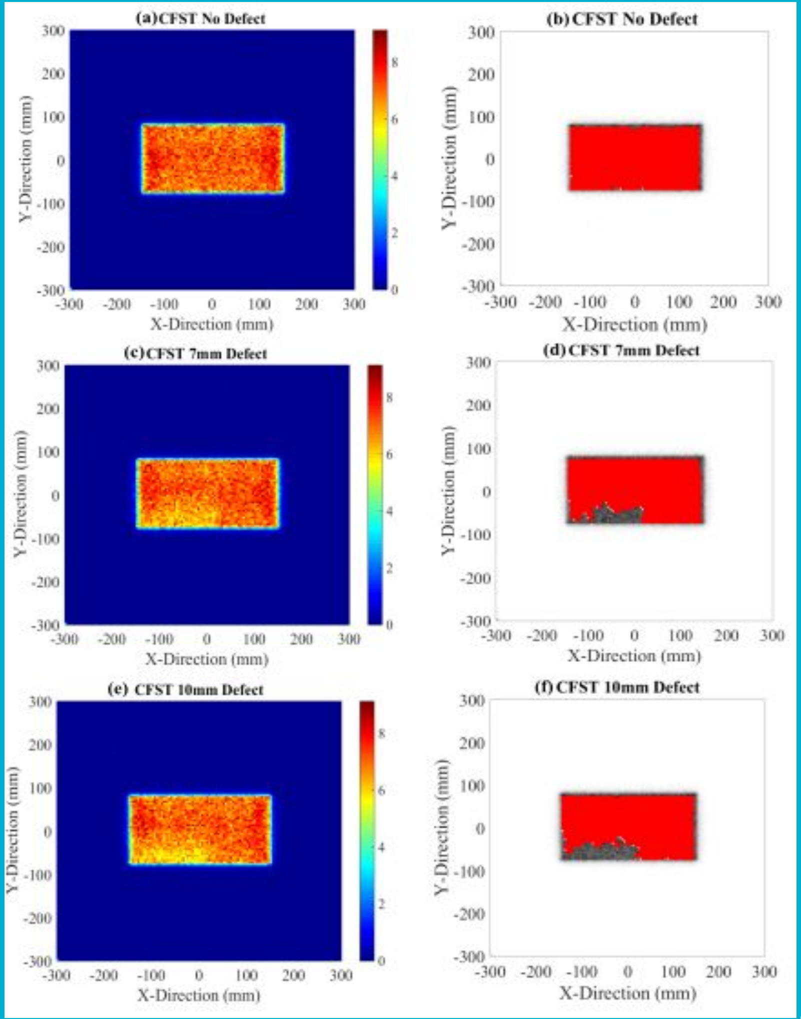

Results: Voids in concrete deck

- Different aspect: only concrete & void (air), instead of 3 (earlier case)
- But low ρ & X_0 cause blurring.
- Shape detection of voids clear in case of 6 cm void.
- Voids at different depths identifiable.
- The defects have been identified with > **4σ** with t-statistics and > **$2\delta n$** from the without-defect case. table

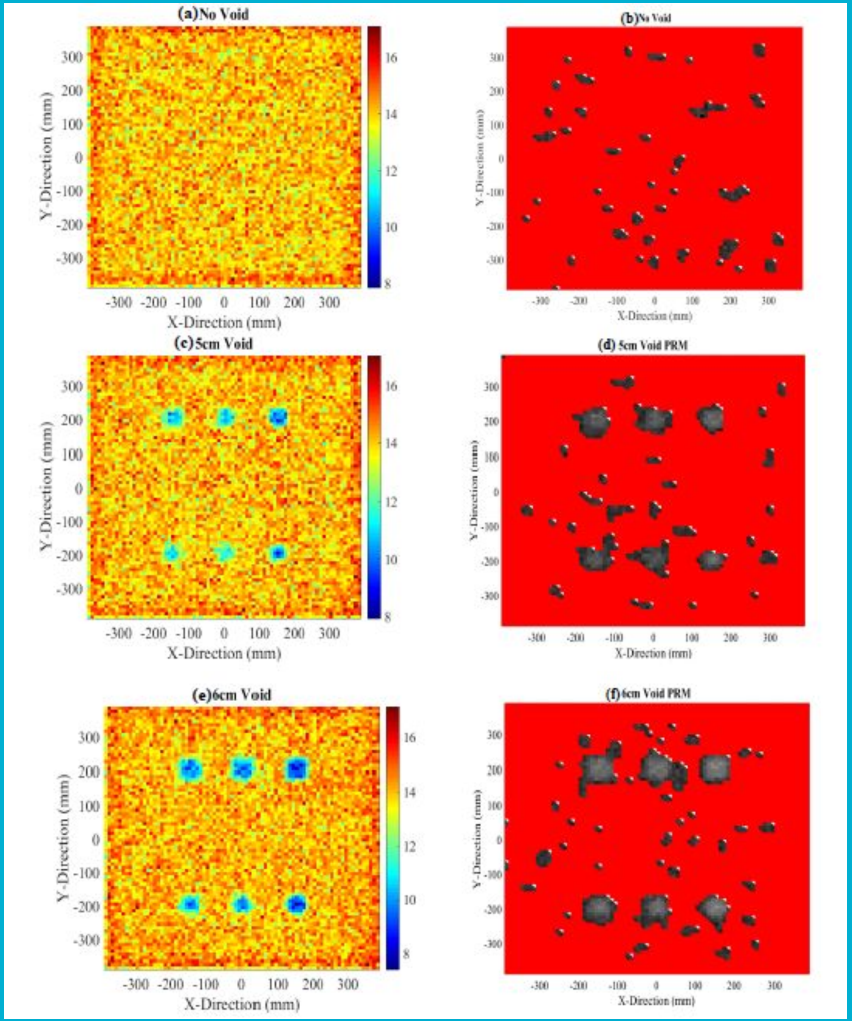

Results: Discrimination results in all 3 cases

Target Type	Defect Dimension (mm)	t-score	p-value	Statistical significance	PRM-score
Rebar	2.25	-2.28	1e-2	2.29	1.48
	4.5	-4.76	1e-6	4.75	1.78
CFST	7	-3.83	6e-5	3.83	3.85
	10	-6.5	4e-11	6.48	4.95
Void	50	-4.07	2e-5	4.2	2.55
	60	-4.88	5e-7	4.89	3.61

Results: Variations with defect thickness and muon exposure

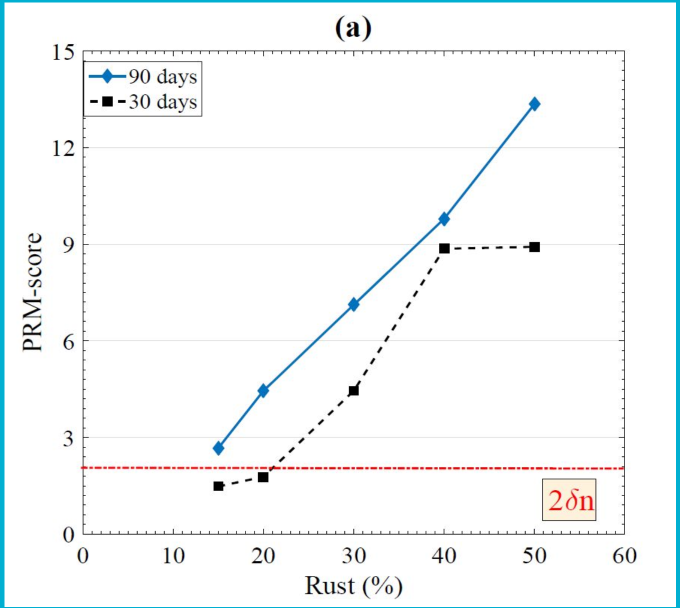

(a) PRM -score

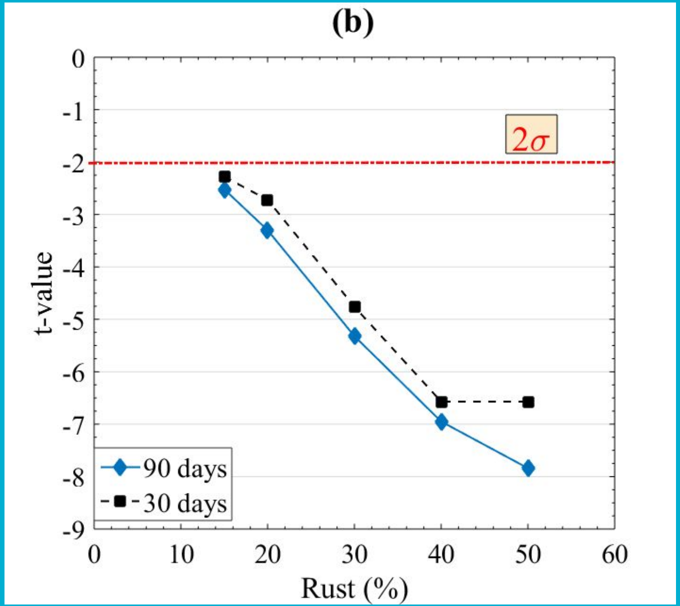

(b)t-value

Limit of discrimination capablity of MST in concrete structure studied.

- ➔ With increased defect thickness discrimination improves.
- ➔ Identification of defects improves with increasing muon exposure.

Conclusion

- MST has been studied as an NDE technique for application in concrete structures.
- Three unique and crucial problems have been studied.
- PRM devised based on scattering parameter and thickness information of sample used for these problems.
- Imaging results have been evaluated using statistical test and PRM-score.
- Reliability of MST studied on the basis of presence of variable materials, different defect size & shape, depth of the defect and exposure.
- Experimental work using detector, readout-DAQ is underway.

Our-Group

These works have been done with

Jaydeep Datta, Nayana Majumdar, Supratik Mukhopadhyay

Saha Institute of Nuclear Physics, Kolkata, India
Homi Bhabha National Institute, Mumbai, India

The work has been arxived: arXiv:2102.08913

Thank You!

Back-up

Overview: MST in concrete Applications (some observations)

Pros	Cons
➔ Natural omnipresent particles available source, non-hazardous. (unlike X-ray and gamma ray imaging.) ➔ Cost effective, free source, only detector handling cost (unlike IR thermography, ultrasonics, gpr) ➔ Independent of weather and other environmental parameters (thermography gets terribly affected.) ➔ Deep penetration power hence used in absorption radiography as well. (Most NDEs can't accurately penetrate ~10 cm) ➔ Can be deployed for larger area imaging. ➔ Detect Changes in target material (based on Z and ρ) ➔ Fast processing time. (Due to low rate, data selection and transfer online.)	➔ Moderate flux (1/cm^2/min). More vertical than horizontal follows $\cos^2\theta$. ➔ Vast energy range (10 MeV-100 GeV), high-scattering may result from large low-Z or small high-Z target. ➔ Very high exposure required for accuracy. ➔ Thin/small defects (< 2mm), cracks can not be located. ➔ Better resolution requires precise detectors and costly electronics. ➔ Haven't been studied for long. (Other NDEs like Ultrasonics, IR, gpr etc studied for > 30 yrs.)

Pattern Recognition Method (PRM)

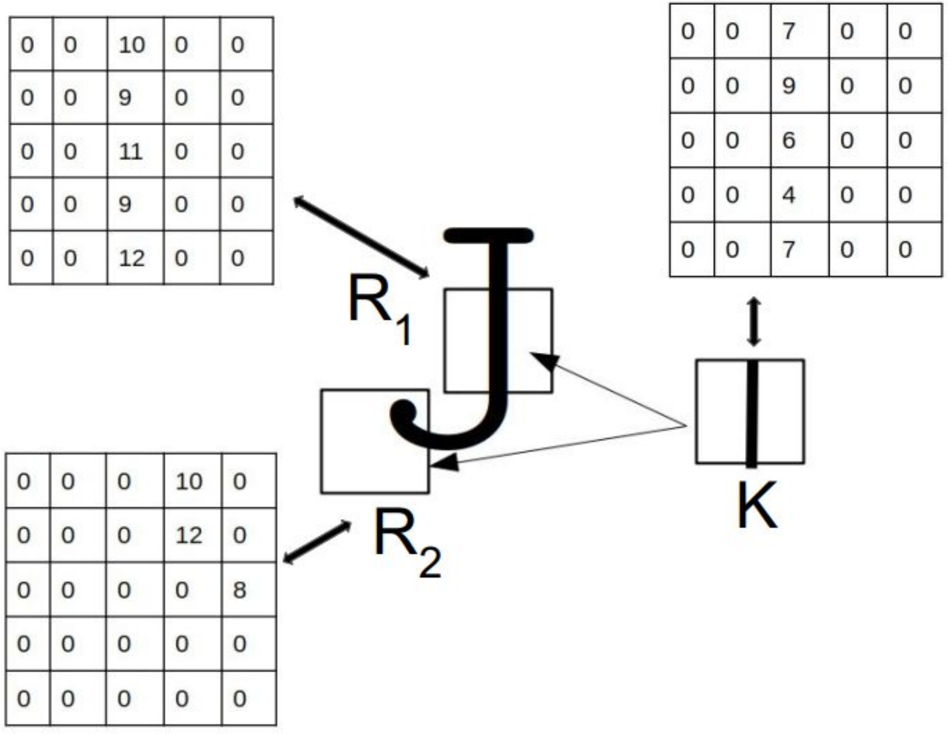

A filter ‘K’ searches for a similar pattern ‘R_1’.

- ROI pixelized in terms of a matrix
- **PRM** searches for similarity with sample in the test image.
- Learning parameter ρ_c.
- Helps Identify Position, Dimension, Shape
- Size of Kernel and pixel user decision

$$R_1{*}K : 7 * 10 + 9 * 9 + 6 * 11 + 4 * 9 + 7 * 12 = 337$$

$$R_2{*}K : 7 * 0 + 9 * 0 + 6 * 0 + 4 * 0 + 7 * 0 = 0$$

JINST 15 (2020) 06, P06029

Pattern Recognition Method (PRM)

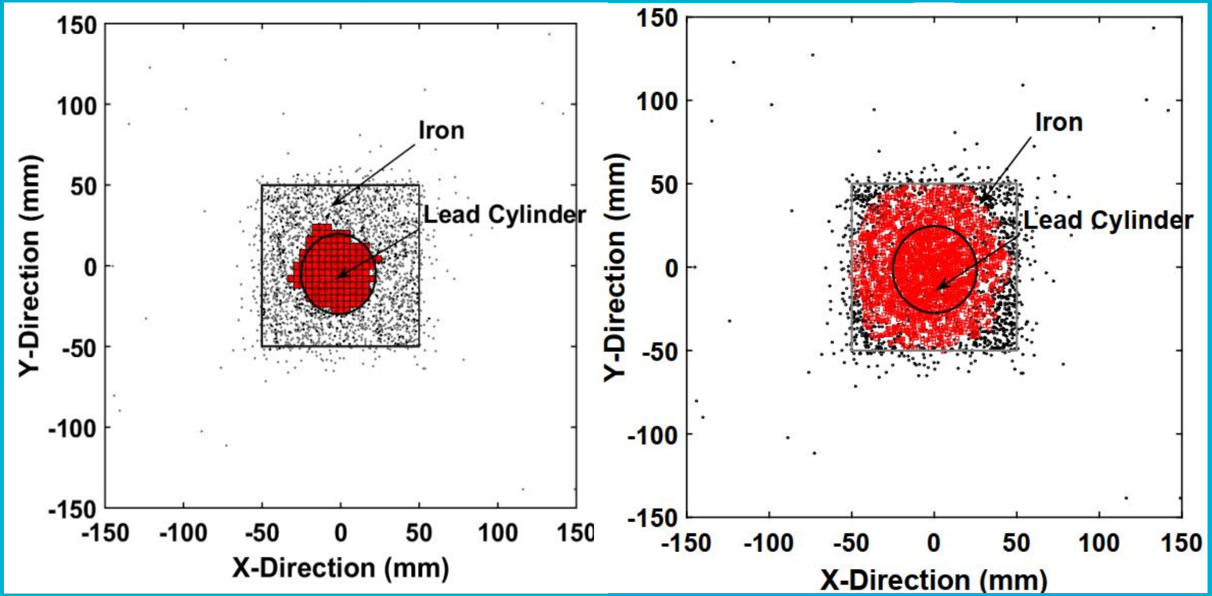

PRM

DBSCAN

- Fe: 10X10X5 cm^3
  Pb: 5 cm dia
- PRM performs better than DBSCAN in complicated scenario.
- Smaller pixel size and kernel required to identify shape

JINST 15 (2020) 06, P06029